



# Mechanical buckling of a functionally graded cylindrical shell with axial and circumferential stiffeners using the third-order shear deformation theory



Hossein Farahani <sup>a,\*</sup>, Reza Azarafza <sup>b</sup>, Farzan Barati <sup>c</sup>

<sup>a</sup> Department of Mechanics, College of Engineering, Hamedan Science and Research Branch, Islamic Azad University, Hamedan, Iran

<sup>b</sup> Department of Mechanical Engineering, Malek Ashtar University of Technology, Tehran, Iran

<sup>c</sup> Department of Mechanical Engineering, Islamic Azad University, Hamedan Branch, Hamedan, Iran

## ARTICLE INFO

### Article history:

Received 10 October 2013

Accepted 7 April 2014

Available online 3 July 2014

### Keywords:

Analytical approach

Buckling behavior

Functionally graded circular cylindrical shell

## ABSTRACT

This paper deals with an analytical approach of the buckling behavior of a functionally graded circular cylindrical shell under axial pressure with external axial and circumferential stiffeners. The shell properties are assumed to vary continuously through the thickness direction. Fundamental relations and equilibrium and stability equations are derived using the third-order shear deformation theory. The resulting equations are employed to obtain the closed-form solution for the critical buckling loads. A simply supported boundary condition is considered for both edges of the shell. The comparison of the results of this study with those in the literature validates the present analysis. The effects of material composition (volume fraction exponent), of the number of stiffeners and of shell geometry parameters on the characteristics of the critical buckling load are described. The analytical results are compared and validated using the finite-element method. The results show that the inhomogeneity parameter, the geometry of the shell and the number of stiffeners considerably affect the critical buckling loads.

© 2014 Académie des sciences. Published by Elsevier Masson SAS. All rights reserved.

## 1. Introduction

Stiffened cylindrical shells have found widespread use in modern engineering, especially in aircraft and spacecraft industry. There have been many studies on the stability of cylindrical shells, but closed-form solutions are possible only for the case when all edges are simply supported. Due to the increasing demands for high structural performances, the study of functionally graded materials in structures has received considerable attention in recent years. The buckling and postbuckling of cylindrical shells under combined loading of external pressure and axial compression have been demonstrated by Shen and Chen [1], who studied the interaction of local and overall buckling in stiffened plates and cylindrical shells.

Classical theories developed for thin elastic shells are mostly based on the Love–Kirchhoff assumptions. This theory considers that straight lines normal to the undeformed middle surface remain straight and normal to the deformed middle surface, that the normal stresses perpendicular to the middle surface can be neglected in stress–strain relationships, and that the transverse displacement is independent of the thickness coordinate. Therefore, transverse shear strains are neglected, as reported in surveys of classical shell theories by Naghdi [2] and Bert [3].

These theories are expected to produce accurate results when the thickness-to-radius ratio ( $h/a$ ) is small. The application of such theories to thick or moderately thick or laminated composite shells can lead to serious errors in deflection or

\* Corresponding author.

stresses. The effect of transverse shear and normal stresses in shells has been studied by Reissner [4]. The effect of transverse shear deformation was also considered by Vinson [5], Dong et al. [6,7], and Reddy [8] extended Vlasov's theory to laminated composite plates and shells. This higher-order theory based on five degrees of freedom (same number as in a first-order shear-deformation theory by Reddy [9]). This theory assumes a constant transverse deflection through the thickness and the displacements of the middle surface expanded as cubic functions of the thickness coordinate. The displacement field leads to a parabolic distribution of the transverse shear stresses and zero transverse normal strain. Therefore, no shear correction was used.

Stiffened cylindrical shells have found widespread use in modern engineering, especially in aircraft and spacecraft industry. There have been many studies on the stability of cylindrical shells, but closed-form solutions are possible only for the case when all edges are simply supported. Due to the increasing demands of high structural performances, the study of functionally graded materials in structures has received considerable attention in recent years.

The buckling and post-buckling of cylindrical shells under the combined loading of external pressure and axial compression has demonstrated by Shen and Chen [10]. An instability analysis of stiffened cylindrical shells under hydrostatic pressure was given by Barush and Singer [11]. The post-buckling of stiffened cylindrical shells under combined external pressure and axial compression was investigated by Shen et al. [12]. Using a novel finite-elements model, Sridharan and Zeggane [13] studied interacting local and overall buckling in stiffened plates and cylindrical shells. Ji Zhen and Yeh Kei [14] studied the part of the cylindrical shell which is stiffened with stringers; it is treated as an isotropic shell, and the part stiffened with rings as a discrete shell element. Based on the Donnell equations, the stability equation of nonhomogeneous cylindrical stiffened shells was obtained by use of the perturbation technique. Sadeghifar et al. [15] studied new buckling results for laminated stiffened cylindrical shells with nonuniform stringers. They used the first-order shear deformation theory to obtain the basic equations.

In this paper, the stability of FG cylindrical shells with axial and circumferential stiffeners was studied. The material properties were assumed to vary smoothly through the shell thickness according to a power-law distribution of the volume fraction of constituent materials. Initially, the stability equations were derived from the third-order shear deformation theory (TSDT). The resulting equations were employed to obtain the critical buckling loads. Also the effects of geometrical parameters, of the number of stiffeners and of the FG power index on the critical buckling load have been studied.

## 2. Formulation

Consider an FG cylindrical shell which is stiffened by external axial and circumferential stiffeners as shown in Fig. 1.

Throughout the current investigation,  $x$ ,  $y$  and  $z$  coordinates coincide with the directions of the length, circumference and thickness of the FG cylinder, respectively.

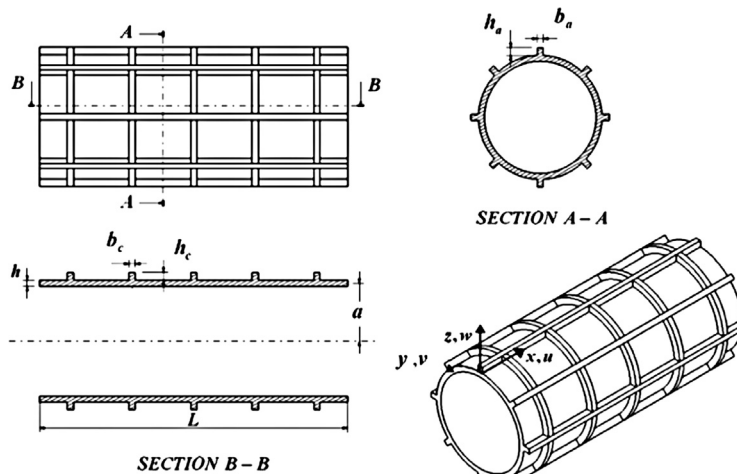


Fig. 1. Geometry and coordinate system of the stiffened cylindrical shell.

The FGM shell being made of a combined ceramic–metal material, the material distribution governed by the equation:

$$V_m(z) = \left( \frac{1}{2} + \frac{z}{h} \right)^\xi, \quad V_c(z) = 1 - V_m(z) \quad (1)$$

where  $V(z)$  is the volume fraction of a constituent material,  $\xi$  is a non-negative volume fraction exponent, and subscripts  $c$  and  $m$  stand for ceramic and metal. Thus, the effective Young modulus of the shell assumed to vary as a power law of the thickness coordinate:

$$E(z) = E_c + E_{mc} \left( \frac{1}{2} + \frac{z}{h} \right)^\xi, \quad E_{mc} = E_m - E_c \tag{2}$$

The material composition varies smoothly from the metal-rich outer surface ( $z = h/2$ ) of the FGM shell to the ceramic-rich inner surface ( $z = -h/2$ ). The displacement fields can be written as:

$$\begin{aligned} u(x, y, z) &= u_0(x, y) + z\varphi_x(x, y) - c_1 z^3(\varphi_x + w_{0,x}) \\ v(x, y, z) &= v_0(x, y) + z\varphi_y(x, y) - c_1 z^3(\varphi_y + w_{0,y}) \\ w(x, y, z) &= w_0(x, y) \end{aligned} \tag{3}$$

where  $u, v$  and  $w$  are displacements of arbitrary points through the cylindrical shell along coordinates  $(x, y, z)$ , and  $c_1$  is equal to  $4/3h^2$ . The kinematic relations for a cylindrical shell are defined by:

$$\begin{aligned} \begin{Bmatrix} \varepsilon_{xx} \\ \varepsilon_{yy} \\ \gamma_{xy} \end{Bmatrix} &= \begin{Bmatrix} \varepsilon_{xx}^{(0)} \\ \varepsilon_{yy}^{(0)} \\ \gamma_{xy}^{(0)} \end{Bmatrix} + z \begin{Bmatrix} \varepsilon_{xx}^{(1)} \\ \varepsilon_{yy}^{(1)} \\ \gamma_{xy}^{(1)} \end{Bmatrix} + z^3 \begin{Bmatrix} \varepsilon_{xx}^{(3)} \\ \varepsilon_{yy}^{(3)} \\ \gamma_{xy}^{(3)} \end{Bmatrix} \\ \begin{Bmatrix} \gamma_{xz} \\ \gamma_{yz} \end{Bmatrix} &= \begin{Bmatrix} \gamma_{xz}^{(0)} \\ \gamma_{yz}^{(0)} \end{Bmatrix} + z^2 \begin{Bmatrix} \gamma_{xz}^{(2)} \\ \gamma_{yz}^{(2)} \end{Bmatrix} \end{aligned}$$

and

$$\begin{aligned} \begin{Bmatrix} \gamma_{xz}^{(0)} \\ \gamma_{yz}^{(0)} \end{Bmatrix} &= \begin{Bmatrix} \varphi_x + w_{0,x} \\ \varphi_y + w_{0,y} \end{Bmatrix} \\ \begin{Bmatrix} \gamma_{xz}^{(2)} \\ \gamma_{yz}^{(2)} \end{Bmatrix} &= -3c_1 \begin{Bmatrix} \varphi_x + w_{0,x} \\ \varphi_y + w_{0,y} \end{Bmatrix} \\ \begin{Bmatrix} \varepsilon_{xx}^{(0)} \\ \varepsilon_{yy}^{(0)} \\ \gamma_{xy}^{(0)} \end{Bmatrix} &= \begin{Bmatrix} u_{0,x} + \frac{w_{0,x}^2}{2} \\ v_{0,y} + \frac{w_{0,y}^2}{2} \\ u_{0,y} + v_{0,x} + w_{0,x}w_{0,y} \end{Bmatrix} \\ \begin{Bmatrix} \varepsilon_{xx}^{(1)} \\ \varepsilon_{yy}^{(1)} \\ \gamma_{xy}^{(1)} \end{Bmatrix} &= \begin{Bmatrix} \varphi_{x,x} \\ \varphi_{y,y} \\ \varphi_{x,y} + \varphi_{y,x} \end{Bmatrix} \\ \begin{Bmatrix} \varepsilon_{xx}^{(3)} \\ \varepsilon_{yy}^{(3)} \\ \gamma_{xy}^{(3)} \end{Bmatrix} &= -c_1 \begin{Bmatrix} \varphi_{x,x} + w_{0,xx} \\ \varphi_{y,y} + w_{0,yy} \\ \varphi_{x,y} + \varphi_{y,x} + 2w_{0,xy} \end{Bmatrix} \end{aligned} \tag{4}$$

Hook's law is defined by:

$$\begin{aligned} \sigma_{xx} &= \frac{E}{(1-\nu^2)}(\varepsilon_{xx} + \nu\varepsilon_{yy}), & \sigma_{yy} &= \frac{E}{(1-\nu^2)}(\varepsilon_{yy} + \nu\varepsilon_{xx}), \\ \tau_{xy} &= \frac{E}{2(1+\nu)}\gamma_{xy}, & \tau_{yz} &= \frac{E}{2(1+\nu)}\gamma_{yz} \end{aligned} \tag{5}$$

The stress resultants are presented as:

$$\begin{aligned} (N_i, M_i, P_i) &= \int_{-\frac{h}{2}}^{\frac{h}{2}} \sigma_i(1, z, z^2) dz, \quad i = xx, yy \\ (N_i, M_i, P_i) &= \int_{-\frac{h}{2}}^{\frac{h}{2}} \tau_i(1, z, z^2) dz, \quad i = xy \end{aligned}$$

$$(Q_i, R_i) = \int_{-\frac{h}{2}}^{\frac{h}{2}} \tau_i(1, z^2) dz, \quad i = xz, yz \quad (6)$$

Substituting Eqs. (4) and (5) into Eq. (6) gives the stress resultants as:

$$\begin{aligned} \begin{Bmatrix} N_{xx} \\ M_{xx} \\ P_{xx} \end{Bmatrix} &= \frac{1}{1-\nu^2} \left( \begin{Bmatrix} A \\ B \\ C \end{Bmatrix} (\varepsilon_{xx}^{(0)} + \nu \varepsilon_{yy}^{(0)}) + \begin{Bmatrix} B \\ D \\ F \end{Bmatrix} (\varepsilon_{xx}^{(1)} + \nu \varepsilon_{yy}^{(1)}) + \begin{Bmatrix} D \\ F \\ G \end{Bmatrix} (\varepsilon_{xx}^{(3)} + \nu \varepsilon_{yy}^{(3)}) \right) \\ \begin{Bmatrix} N_{yy} \\ M_{yy} \\ P_{yy} \end{Bmatrix} &= \frac{1}{1-\nu^2} \left( \begin{Bmatrix} A \\ B \\ C \end{Bmatrix} (\varepsilon_{yy}^{(0)} + \nu \varepsilon_{xx}^{(0)}) + \begin{Bmatrix} B \\ D \\ F \end{Bmatrix} (\varepsilon_{yy}^{(1)} + \nu \varepsilon_{xx}^{(1)}) + \begin{Bmatrix} D \\ F \\ G \end{Bmatrix} (\varepsilon_{yy}^{(3)} + \nu \varepsilon_{xx}^{(3)}) \right) \\ \begin{Bmatrix} N_{xy} \\ M_{xy} \\ P_{xy} \end{Bmatrix} &= \frac{1}{2(1+\nu)} \left( \begin{Bmatrix} A \\ B \\ C \end{Bmatrix} \gamma_{xy}^{(0)} + \begin{Bmatrix} B \\ D \\ F \end{Bmatrix} \gamma_{xy}^{(1)} + \begin{Bmatrix} D \\ F \\ G \end{Bmatrix} \gamma_{xy}^{(3)} \right) \\ \begin{Bmatrix} Q_{xz} \\ R_{xz} \end{Bmatrix} &= \frac{1}{2(1+\nu)} \left( \begin{Bmatrix} A \\ C \end{Bmatrix} \gamma_{xz}^{(0)} + \begin{Bmatrix} C \\ F \end{Bmatrix} \gamma_{xz}^{(2)} \right) \\ \begin{Bmatrix} Q_{yz} \\ R_{yz} \end{Bmatrix} &= \frac{1}{2(1+\nu)} \left( \begin{Bmatrix} A \\ C \end{Bmatrix} \gamma_{yz}^{(0)} + \begin{Bmatrix} C \\ F \end{Bmatrix} \gamma_{yz}^{(2)} \right) \end{aligned} \quad (7)$$

where  $A, B, C, D, F$  and  $G$  are given by:

$$(A, B, C, D, F, G) = \int_{-\frac{h}{2}}^{\frac{h}{2}} (1, z, z^2, z^3, z^4, z^6) E(x, z) dz \quad (8)$$

The strain energy of the shell,  $U_{sh}$ , may be written as:

$$U_{sh} = \frac{1}{2} \int_0^L \int_0^{2\pi a} \int_{-h/2}^{h/2} (\sigma_{xx} \varepsilon_{xx} + \sigma_{yy} \varepsilon_{yy} + \tau_{xy} \gamma_{xy} + \tau_{xz} \gamma_{xz} + \tau_{yz} \gamma_{yz}) dz dy dx \quad (9)$$

Assuming a constant contact between circumferential and axial stiffeners, the latter are assumed to behave like beam elements. The kinematic description of the beam elements is based on the Euler–Bernoulli beam theory and can be written under the form (see [16, p. 798]):

$$\begin{aligned} v_c(x, y, z) &= v_1(x, y) - z \frac{\partial w_1}{\partial y} \\ w_c(x, y, z) &= w_1(x, y) \\ u_a(x, y, z) &= u_1(x, y) - z \frac{\partial w_1}{\partial x} \\ w_a(x, y, z) &= w_1(x, y) \end{aligned} \quad (10)$$

$$\quad (11)$$

where,  $(u_c, w_c)$  and  $(v_a, w_a)$  are circumferential and axial stiffeners displacements, respectively, and  $(u_1, v_1, w_1)$  show the displacement components of the point which are located on the surface of the shell. The kinematic relations for the circumferential stiffeners can be written as [16]:

$$\begin{aligned} \varepsilon_a &= \frac{\partial u_1}{\partial x} + \frac{1}{2} \left( \frac{\partial w_1}{\partial x} \right)^2 - z \left( \frac{\partial^2 w_1}{\partial x^2} \right) \\ \varepsilon_c &= \frac{\partial v_1}{\partial y} + \frac{1}{2} \left( \frac{\partial w_1}{\partial y} \right)^2 + \frac{w_1}{a} - z \left( \frac{\partial^2 w_1}{\partial y^2} \right) \end{aligned} \quad (12)$$

Hook's law is defined for stiffeners by:

$$\sigma_a = E_a \varepsilon_a, \quad \sigma_c = E_c \varepsilon_c \quad (13)$$

The potential energy of axial stiffeners is [13]:

$$\begin{aligned}
 U_a &= \frac{1}{2S_a} \int_0^L \int_0^{2\pi a} \left( \int_{A_a} \sigma_a \varepsilon_a dA + G_a J_a \left( \frac{\partial^2 w_1}{\partial x \partial y} \right)^2 \right) dx dy \\
 &= \frac{1}{2S_a} \int_0^L \int_0^{2\pi a} \left\{ E_a A_a \left( \frac{\partial u_1}{\partial x} + \frac{1}{2} \left( \frac{\partial w_1}{\partial x} \right)^2 \right)^2 + E_a I_a \left( \frac{\partial^2 w_1}{\partial x^2} \right)^2 - 2\bar{Z}_a A_a E_a \left( \frac{\partial^2 w_1}{\partial x^2} \right) \left( \frac{\partial u_1}{\partial x} + \frac{1}{2} \left( \frac{\partial w_1}{\partial x} \right)^2 \right) \right. \\
 &\quad \left. + G_a J_a \left( \frac{\partial^2 w_1}{\partial x \partial y} \right)^2 \right\} dx dy
 \end{aligned} \tag{14}$$

and the potential energy for circumferential stiffeners is:

$$\begin{aligned}
 U_c &= \frac{1}{2S_c} \int_0^L \int_0^{2\pi a} \left( \int_{A_c} \sigma_c \varepsilon_c dA + G_c J_c \left( \frac{\partial^2 w_1}{\partial x \partial y} \right)^2 \right) dx dy \\
 &= \frac{1}{2S_c} \int_0^L \int_0^{2\pi a} \left\{ E_c A_c \left( \frac{\partial v_1}{\partial y} + \frac{w_1}{a} + \frac{1}{2} \left( \frac{\partial w_1}{\partial y} \right)^2 \right)^2 + E_c I_c \left( \frac{\partial^2 w_1}{\partial y^2} \right)^2 \right. \\
 &\quad \left. - 2\bar{Z}_c A_c E_c \left( \frac{\partial^2 w_1}{\partial y^2} \right) \left( \frac{\partial v_1}{\partial y} + \frac{w_1}{a} + \frac{1}{2} \left( \frac{\partial w_1}{\partial y} \right)^2 \right) + G_c J_c \left( \frac{\partial^2 w_1}{\partial x \partial y} \right)^2 \right\} dx dy
 \end{aligned} \tag{15}$$

where subscripts c and a stand for circumferential and axial stiffeners,  $A$  is the area of the stiffener,  $I$  is the moment of inertia of the stiffener about the reference surface ( $z=0$ ),  $\bar{Z}$  is the distance from the stiffener to the reference surface,  $J$  is the torsional constant and  $E_c$  and  $E_a$  are the Young modulus of the circumferential and axial stiffeners, respectively. Here  $S_a$  and  $S_c$  are the distances between the circumferential and axial stiffeners, respectively, and are defined by:

$$\begin{aligned}
 S_a &= 2\pi a / N_a \\
 S_c &= L / N_c
 \end{aligned} \tag{16}$$

where  $N_a$  and  $N_c$  are the numbers of axial and circumferential stiffeners, respectively.

The total potential energy of a cylindrical shell subjected to the axial pressure loading is defined as:

$$V = U + \Omega \tag{17}$$

The total strain energy for cylindrical shell and stiffeners is obtained as follows:

$$U = U_{sh} + U_a + U_c \tag{18}$$

The potential energy of the applied loads,  $\Omega$ , for a conservative system is the negative of the work done by loads as the structure deformed. Thus, for the axial compressive edge load,  $P$ , it is defined by:

$$\Omega = \int_0^L \int_0^{2\pi a} \frac{1}{2\pi a} P \frac{\partial u}{\partial x} dy dx \tag{19}$$

Using the minimum potential energy criterion [17], the equilibrium equations of the stiffened cylindrical shell composed of functionally graded materials is obtained as:

$$\begin{aligned}
 \frac{\partial N_{xx}}{\partial x} + \frac{\partial N_{xy}}{\partial y} + \frac{\partial}{\partial x} \left( \frac{1}{S_a} \left( E_a A_a \left( \frac{\partial u_1}{\partial x} + \frac{1}{2} \left( \frac{\partial w_1}{\partial x} \right)^2 \right) - \bar{Z}_a E_a A_a \frac{\partial^2 w_1}{\partial x^2} \right) \right) &= 0 \\
 \frac{\partial N_{xy}}{\partial x} + \frac{\partial N_{yy}}{\partial y} + \frac{\partial}{\partial y} \left( \frac{1}{S_c} \left( E_c A_c \left( \frac{\partial v_1}{\partial y} + \frac{1}{2} \left( \frac{\partial w_1}{\partial y} \right)^2 + \frac{w_1}{a} \right) - \bar{Z}_c E_c A_c \frac{\partial^2 w_1}{\partial y^2} \right) \right) &= 0 \\
 \frac{\partial Q_{xz}}{\partial x} + \frac{\partial Q_{yz}}{\partial y} - 3c_1 \left( \frac{\partial R_{xz}}{\partial x} + \frac{\partial R_{yz}}{\partial y} \right) + c_1 \left( \frac{\partial^2 P_{xx}}{\partial x^2} + 2 \frac{\partial^2 P_{xy}}{\partial x \partial y} + \frac{\partial^2 P_{yy}}{\partial y^2} \right) - \frac{1}{a} N_{yy} \\
 + N_{xx} \frac{\partial^2 w_0}{\partial x^2} + 2N_{xy} \frac{\partial^2 w_0}{\partial x \partial y} + N_{yy} \frac{\partial^2 w_0}{\partial y^2} + \frac{1}{S_c} \bar{N}_{yy} \frac{\partial^2 w_1}{\partial y^2} + \frac{1}{S_a} \bar{N}_{xx} \frac{\partial^2 w_1}{\partial x^2} &= 0
 \end{aligned}$$

$$\begin{aligned}
& -\frac{1}{aS_c} \left( E_c A_c \left( \frac{\partial v_1}{\partial y} + \frac{1}{2} \left( \frac{\partial w_1}{\partial y} \right)^2 + \frac{w_1}{a} \right) - E_c A_c \bar{Z}_c \frac{\partial^2 w_1}{\partial y^2} \right) - \frac{\partial^2}{\partial y^2} \left( \frac{1}{S_c} \left( (E_c I_c + \bar{Z}_c E_c A_c c_1 (h/2)^3) \right. \right. \\
& \times \left. \left. \frac{\partial^2 w_1}{\partial y^2} - (\bar{Z}_c E_c A_c + c_1 (h/2)^3) \left( \frac{\partial v_1}{\partial y} + \frac{1}{2} \left( \frac{\partial w_1}{\partial y} \right)^2 + \frac{w_1}{a} \right) \right) \right) - \frac{\partial^2}{\partial x^2} \left( \frac{1}{S_a} \left( (E_a I_a + \bar{Z}_a E_a A_a c_1 (h/2)^3) \frac{\partial^2 w_1}{\partial x^2} \right. \right. \\
& \left. \left. - (\bar{Z}_a E_a A_a + c_1 h^3) \left( \frac{\partial u_1}{\partial x} + \frac{1}{2} \left( \frac{\partial w_1}{\partial x} \right)^2 \right) \right) \right) = 0 \\
& \frac{\partial M_{xx}}{\partial x} + \frac{\partial M_{xy}}{\partial y} - Q_{xz} + 3c_1 R_{xz} - c_1 \left( \frac{\partial P_{xx}}{\partial x} + \frac{\partial P_{xy}}{\partial y} \right) \\
& + \frac{\partial}{\partial x} \left( \frac{1}{S_a} \left( (h/2) - c_1 (h/2)^3 \right) E_a A_a \left( \frac{\partial u_1}{\partial x} + \frac{1}{2} \left( \frac{\partial w_1}{\partial x} \right)^2 \right) - \bar{Z}_a E_a A_a (h/2) - c_1 (h/2)^3 \right) \left( \frac{\partial w_1}{\partial x} \right) \right) = 0 \\
& \frac{\partial M_{xy}}{\partial x} + \frac{\partial M_{yy}}{\partial y} - Q_{yz} + 3c_1 R_{yz} - c_1 \left( \frac{\partial P_{xy}}{\partial x} + \frac{\partial P_{yy}}{\partial y} \right) \\
& + \frac{\partial}{\partial y} \left( \frac{1}{S_c} \left( (h/2) - c_1 (h/2)^3 \right) E_c A_c \left( \frac{\partial v_1}{\partial y} + \frac{1}{2} \left( \frac{\partial w_1}{\partial y} \right)^2 + \frac{w_1}{a} \right) - \frac{1}{S_c} \bar{Z}_c E_c A_c \left( (h/2) - c_1 (h/2)^3 \right) \left( \frac{\partial w_1}{\partial y} \right) \right) = 0
\end{aligned} \tag{20}$$

where  $\bar{N}_{xx}$  and  $\bar{N}_{yy}$  are defined by:

$$\begin{aligned}
\bar{N}_{xx} &= \int_{A_a} \sigma_a dA = \int_{h/2}^{h/2+h_f} b_a \sigma_a dz \\
&= E_a A_a \left( \frac{\partial u_1}{\partial x} + \frac{1}{2} \left( \frac{\partial w_1}{\partial x} \right)^2 \right) - \bar{Z}_a E_a A_a \left( \frac{\partial^2 w_1}{\partial x^2} \right) \\
\bar{N}_{yy} &= \int_{A_c} \sigma_c dA = \int_{h/2}^{h/2+h_f} b_c \sigma_c dz \\
&= E_c A_c \left( \frac{\partial v_1}{\partial y} + \frac{1}{2} \left( \frac{\partial w_1}{\partial y} \right)^2 + \frac{w_1}{a} \right) - \bar{Z}_c E_c A_c \left( \frac{\partial^2 w_1}{\partial y^2} \right)
\end{aligned} \tag{21}$$

The stability equations of the cylindrical shell may be derived by the variational approach. If  $V$  is the total potential energy of the shell, the first variation,  $\delta V$ , is associated with the state of equilibrium. The stability of the original configuration of the shell around the equilibrium state can be determined by the sign of second variation,  $\delta^2 V$ . However, the condition  $\delta^2 V = 0$  is used to derive the stability equations of many practical problems concerning the buckling of shells [17]. Thus, the stability equations are represented by the Euler equations for the integrand in the second variation expression:

$$\begin{aligned}
& \frac{\partial N_{xx}^1}{\partial x} + \frac{\partial N_{xy}^1}{\partial y} + \frac{\partial}{\partial x} \left( \frac{1}{S_a} \left( E_a A_a \left( \frac{\partial u_1^1}{\partial x} + \frac{1}{2} \left( \frac{\partial w_1^1}{\partial x} \right)^2 \right) - \bar{Z}_a E_a A_a \frac{\partial^2 w_1^1}{\partial x^2} \right) \right) = 0 \\
& \frac{\partial N_{xy}^1}{\partial x} + \frac{\partial N_{yy}^1}{\partial y} + \frac{\partial}{\partial y} \left( \frac{1}{S_c} \left( E_c A_c \left( \frac{\partial v_1^1}{\partial y} + \frac{1}{2} \left( \frac{\partial w_1^1}{\partial y} \right)^2 + \frac{w_1^1}{a} \right) - \bar{Z}_c E_c A_c \frac{\partial^2 w_1^1}{\partial y^2} \right) \right) = 0 \\
& \frac{\partial Q_{xz}^1}{\partial x} + \frac{\partial Q_{yz}^1}{\partial y} - 3c_1 \left( \frac{\partial R_{xz}^1}{\partial x} + \frac{\partial R_{yz}^1}{\partial y} \right) + c_1 \left( \frac{\partial^2 P_{xx}^1}{\partial x^2} + 2 \frac{\partial^2 P_{xy}^1}{\partial x \partial y} + \frac{\partial^2 P_{yy}^1}{\partial y^2} \right) - \frac{1}{a} N_{yy}^1 + N_{xx}^0 \frac{\partial^2 w_0}{\partial x^2} + 2N_{xy}^0 \frac{\partial^2 w_0}{\partial x \partial y} \\
& + N_{yy}^0 \frac{\partial^2 w_0^1}{\partial y^2} + \frac{1}{S_c} \bar{N}_{yy}^0 \frac{\partial^2 w_1^1}{\partial y^2} + \frac{1}{S_a} \bar{N}_{xx}^0 \frac{\partial^2 w_1^1}{\partial x^2} - \frac{1}{aS_c} \left( E_c A_c \left( \frac{\partial v_1^1}{\partial y} + \frac{1}{2} \left( \frac{\partial w_1^1}{\partial y} \right)^2 + \frac{w_1^1}{a} \right) - E_c A_c \bar{Z}_c \frac{\partial^2 w_1^1}{\partial y^2} \right) \\
& - \frac{\partial^2}{\partial y^2} \left( \frac{1}{S_c} \left( (E_c I_c + \bar{Z}_c E_c A_c c_1 (h/2)^3) \frac{\partial^2 w_1^1}{\partial y^2} \right) - (\bar{Z}_c E_c A_c + c_1 (h/2)^3) \left( \frac{\partial v_1^1}{\partial y} + \frac{1}{2} \left( \frac{\partial w_1^1}{\partial y} \right)^2 + \frac{w_1^1}{a} \right) \right) \\
& - \frac{\partial^2}{\partial x^2} \left( \frac{1}{S_a} \left( (E_a I_a + \bar{Z}_a E_a A_a c_1 (h/2)^3) \frac{\partial^2 w_1^1}{\partial x^2} \right) - (\bar{Z}_a E_a A_a + c_1 (h/2)^3) \left( \frac{\partial u_1^1}{\partial x} + \frac{1}{2} \left( \frac{\partial w_1^1}{\partial x} \right)^2 \right) \right) = 0 \\
& \frac{\partial M_{xx}^1}{\partial x} + \frac{\partial M_{xy}^1}{\partial y} - Q_{xz}^1 + 3c_1 R_{xz}^1 - c_1 \left( \frac{\partial P_{xx}^1}{\partial x} + \frac{\partial P_{xy}^1}{\partial y} \right) + \frac{\partial}{\partial x} \left( \frac{1}{S_a} \left( (h/2) - c_1 (h/2)^3 \right) E_a A_a \left( \frac{\partial u_1^1}{\partial x} + \frac{1}{2} \left( \frac{\partial w_1^1}{\partial x} \right)^2 \right) \right)
\end{aligned}$$

$$\begin{aligned}
 & -\bar{Z}_a E_a A_a ((h/2) - c_1 (h/2)^3) \left( \frac{\partial w_1^1}{\partial x} \right) = 0 \\
 & \frac{\partial M_{xy}^1}{\partial x} + \frac{\partial M_{yy}^1}{\partial y} - Q_{yz}^1 + 3c_1 R_{yz}^1 - c_1 \left( \frac{\partial P_{xy}^1}{\partial x} + \frac{\partial P_{yy}^1}{\partial y} \right) \\
 & + \frac{\partial}{\partial y} \left( \frac{1}{S_c} ((h/2) - c_1 (h/2)^3) E_c A_c \left( \frac{\partial v_1^1}{\partial y} + \frac{1}{2} \left( \frac{\partial w_1^1}{\partial y} \right)^2 + \frac{w_1^1}{a} \right) - \frac{1}{S_c} \bar{Z}_c E_c A_c ((h/2) - c_1 (h/2)^3) \left( \frac{\partial w_1^1}{\partial y} \right) \right) = 0
 \end{aligned} \tag{22}$$

where  $N_{xx}^0$ ,  $N_{yy}^0$ , and  $N_{xy}^0$  are the pre-buckling force resultants of the shell, and  $\bar{N}_{xx}^0$  and  $\bar{N}_{yy}^0$  are the pre-buckling forces of the stiffeners.

### 3. Buckling analysis

In this section, a closed-form solution for obtaining the critical buckling load is presented. To determine the critical buckling loads, the pre-buckling mechanical forces should be found from the equilibrium equations and then substituted into the stability equations for the buckling analysis. Under a uniformly distributed axial compressive load  $P$ , the cylinder shortens, except at the ends, and increases in diameter. The initial deformation is axisymmetric and the pre-buckling mechanical forces are given by:

$$\begin{aligned}
 N_{yy}^0 &= N_{xy}^0 = \bar{N}_{xx}^0 = \bar{N}_{yy}^0 = 0 \\
 N_{xx}^0 &= -\frac{P}{2\pi a}
 \end{aligned} \tag{23}$$

The simply supported boundary condition is considered for both edges. The displacement field can be defined by:

$$\begin{aligned}
 u_0^1 &= u_{mn} \cos\left(\frac{m\pi x}{L}\right) \sin\left(\frac{ny}{a}\right) \\
 v_0^1 &= v_{mn} \sin\left(\frac{m\pi x}{L}\right) \cos\left(\frac{ny}{a}\right) \\
 w_0^1 &= w_{mn} \sin\left(\frac{m\pi x}{L}\right) \sin\left(\frac{ny}{a}\right) \\
 \varphi_x^1 &= \varphi_{xmn} \cos\left(\frac{m\pi x}{L}\right) \sin\left(\frac{ny}{a}\right) \\
 \varphi_y^1 &= \varphi_{ymn} \sin\left(\frac{m\pi x}{L}\right) \cos\left(\frac{ny}{a}\right) \quad m, n = 1, 2, \dots
 \end{aligned} \tag{24}$$

where  $m$  and  $n$  are the axial and circumferential half-wave numbers, respectively. The simply supported boundary condition at both edges is satisfied. By substituting Eq. (24) into Eq. (22), we obtain the coefficient matrix; then we set the determinant of the coefficient matrix at zero and derive the buckling load as a function of half-wave parameters  $m$  and  $n$ . Using the principle of minimum potential energy and the Ritz method is equivalent to using the matrix equation:

$$\begin{aligned}
 \Pi &= U \Delta U \\
 U &= U_{sh} + U_a + U_c \\
 \delta \Pi &= 0 \\
 \frac{\partial^2 \Pi}{\partial \pi^2} &= 0, \quad \pi = \{A, B, C, D, E\}
 \end{aligned} \tag{25}$$

$$\begin{bmatrix} L_{11} & L_{12} & L_{13} & L_{14} & L_{15} \\ L_{21} & L_{22} & L_{23} & L_{24} & L_{25} \\ L_{31} & L_{32} & L_{33} & L_{34} & L_{35} \\ L_{41} & L_{42} & L_{43} & L_{44} & L_{45} \\ L_{51} & L_{52} & L_{53} & L_{54} & L_{55} \end{bmatrix} \begin{Bmatrix} A \\ B \\ C \\ D \\ E \end{Bmatrix} = \begin{Bmatrix} 0 \\ 0 \\ 0 \\ 0 \\ 0 \end{Bmatrix} \tag{26}$$

$L_{ij}$  are coefficients based on the material's properties and the geometrical parameters (Appendix 1).

We obtain an obvious solution:

$$|L_{ij}| = 0 \tag{27}$$

We obtain a high correlation with the shell buckling equation expressed as follows:

$$\eta_1 N^3 + \eta_2 N^2 + \eta_3 N + \eta_4 = 0 \quad (28)$$

$N$  is the shell buckling load and  $(\eta_i)$  are terms corresponding to coefficients  $(L_{ij})$ .

The critical buckling load may be determined by minimizing the buckling load with  $m$  and  $n$ . The critical buckling load is the smallest buckling load.

#### 4. Calculation results and discussion

A ceramic–metal FG stiffened cylindrical shell is considered. The basic materials properties determined at room temperature (300 K) are displayed in Table 1.

**Table 1**  
Basic properties of the materials at room temperature.

Constituents	Material	Young's modulus (GPa)
Ceramic	Al <sub>2</sub> O <sub>3</sub>	300
Metal	Al 1100	69

The Poisson ratio is assumed to be constant and equal to 0.3.

As a numerical example, the numbers of axial and circumferential stiffeners are 15 and 20 respectively. Let  $h_a = h_c = b_a = b_c = 1$  mm and  $E_a = E_c = 151$  GPa. The results for an aluminum isotropic shell are [17] listed in Tables 2 and 3. The values of the buckling load for an FG cylindrical shell of thickness-to-radius ratio  $h/a$  and the power law index are listed in Table 4.

**Table 2**  
Critical axial buckling load (MN) for an isotropic shell made of alumina, with  $L/a = 1$  and  $a = 0.3$  m.

		Present	Almroth & Brush [17]
$h/a = 1/30$	Unstiffened	25.8814	26.2390
	Stiffened	25.9558	26.3023
$h/a = 1/50$	Unstiffened	9.4834	9.4460
	Stiffened	9.4776	9.4827
$h/a = 1/100$	Unstiffened	2.3536	2.3615
	Stiffened	2.3743	2.3659
$h/a = 1/200$	Unstiffened	0.5891	0.5904
	Stiffened	0.5999	0.5988
$h/a = 1/300$	Unstiffened	0.2620	0.2623
	Stiffened	0.2686	0.2672

**Table 3**  
Critical axial buckling load (MN) for an isotropic shell made of alumina, compared with the results of ANSYS and of reference [17], with  $L/a = 1$  and  $a = 0.3$  m.

	Present	ANSYS	Almroth & Brush [17]
Critical axial loads (MN)			
$h = 1$ mm	0.2620	0.2610 (0.38%)	0.2623 (0.11%)
$h = 3$ mm	2.3536	2.3260 (1.17%)	2.3615 (0.33%)
$h = 6$ mm	9.4834	9.2381 (1.31%)	9.4460 (0.90%)
$h = 12$ mm	37.1370	36.5216 (1.66%)	37.7841 (1.02%)

**Table 4**  
Critical axial buckling load (MN) for FG cylindrical shells, with  $L/a = 1$  and  $a = 0.3$  m.

		$\xi = 1$	$\xi = 2$	$\xi = 5$
$h/a = 0.002$	Unstiffened	0.2353	0.2798	0.3320
	Stiffened	0.2656	0.3101	0.3615
$h/a = 0.01$	Unstiffened	5.8618	6.9722	8.2729
	Stiffened	5.9351	7.0448	8.3422
$h/a = 0.02$	Unstiffened	23.3595	27.8010	32.9763
	Stiffened	23.4984	27.9373	33.1076

It can be seen that the critical buckling load increases by increasing the FG power index; varying material properties along the thickness of the shell results in an increase in the critical buckling load. Also it is acceptable that by increasing the thickness-to-radius ratio, the critical buckling load increases.

In Fig. 2 the critical buckling load is plotted versus the number of axial and circumferential stiffeners for a stiffened FG shell. It can be seen that the percentage increase in the buckling load rises continuously with the increment of the number of stringers; one may notice that circumferential stiffeners are less effective in stiffening the shell than axial stiffeners.

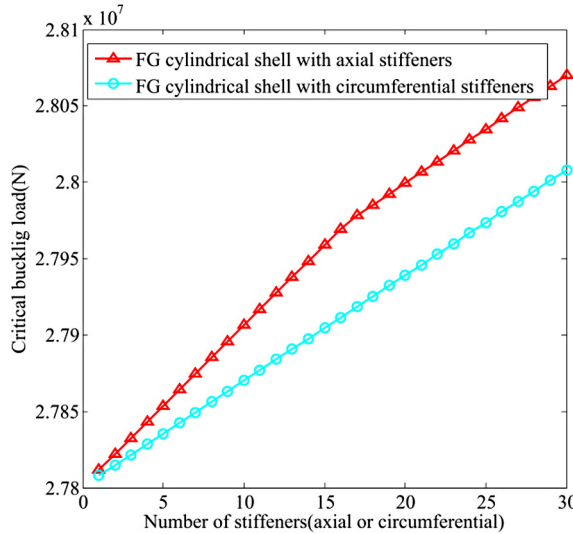


Fig. 2. (Color online.) Critical buckling load as a function of the number of stiffeners for a stiffened FG cylindrical shell, with  $\xi = 2$ ,  $h/a = 0.02$ ,  $L/a = 1$ , and  $a = 0.3$  m.

The variation of the critical buckling load with the length-to-radius ratio,  $L/a$ , for stiffened and unstiffened cylindrical shells is shown in Fig. 3.

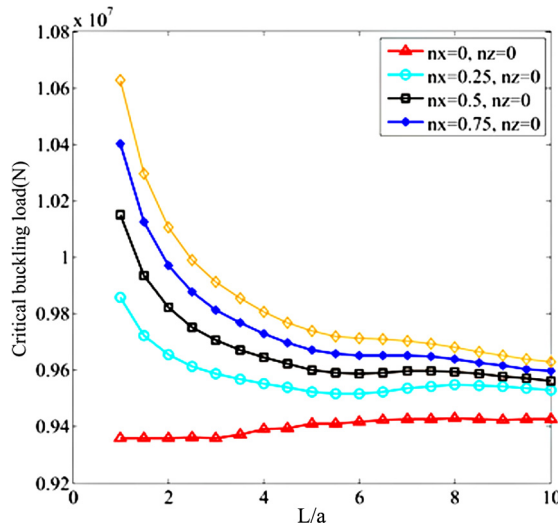


Fig. 3. (Color online.) Critical buckling load as a function of the length-to-radius ratio for a stiffened FG cylindrical shell, with  $h/a = 0.02$  and  $a = 0.3$  m.

The results show that the critical buckling load decreases when increasing the length-to-radius ratio.

The variation of the critical buckling load for a stiffened FG cylindrical shell is exhibited in Fig. 4. Through increasing the power index, the critical buckling load increases as expected. Also the critical buckling loads appear to be constant for high values of the power index.

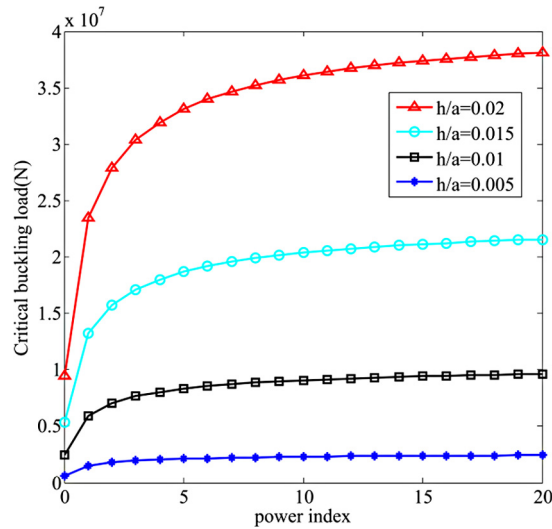


Fig. 4. (Color online.) Critical buckling load as a function of the power index for a stiffened FG power index, with  $N_a = N_c = 15$ ,  $L/a = 1$  and  $a = 0.3$  m.

## 5. Conclusions

In this paper the stability of stiffened FG cylindrical shell is studied. The equilibrium and stability equations are derived based on TSDT. The system of partial differential equations is solved analytically. The effects of the geometrical parameters, the power index and the number of rings on the critical buckling load have been studied. The conclusions can be explained briefly as follows:

- The critical buckling load decreases by increasing the length-to-radius and increases by increasing the thickness-to-radius ratios;
- through increasing the power index, the critical buckling load increases;
- circumferential stiffeners are less effective in stiffening the shell under axial pressure.

## Appendix 1

$$L_{11} = -\left(A_{11}a\alpha^2 T_1 - n^2 \frac{A_{66}}{a} T_2\right) + \frac{1}{2} N_a L \pi \lambda^2 A_a (E_a)$$

$$L_{12} = (A_{12} + A_{66})nT_2$$

$$L_{13} = A_{12}T_2 + \frac{1}{2} N_a L \pi \lambda^3 A_a z_a (E_a)$$

$$L_{14} = B_{11}a\alpha T_1 + \frac{B_{66}}{a} \frac{n^2}{\alpha} T_2$$

$$L_{15} = (B_{12} + B_{66})nT_2$$

$$L_{21} = -(A_{12} + A_{66}) \frac{n}{a}$$

$$L_{22} = A_{66} - \left(\frac{A_{22}}{a^2} \frac{n^2}{\alpha} + \frac{H_{44}}{a^2} \frac{1}{\alpha^2}\right) \frac{T_4}{T_3} + \frac{2n^2 \pi^2 A_c E_c}{a} \sum_{k=1}^{N_c} \sin^2 \lambda x_k + \frac{1}{2} N_a L \pi \lambda_a^2 A_a$$

$$L_{23} = -\left(\frac{H_{44}}{a^2} + \frac{A_{22}}{a^2}\right) \frac{n}{\alpha^2} \frac{T_4}{T_3} - \frac{2n^2 \pi A_c E_c}{a} \sum_{k=1}^{N_c} \sin^2 \lambda x_k - \frac{N_a L n \pi A_a z_a \lambda^2 N_a}{2a}$$

$$- \frac{2n^3 \pi^2 A_c z_c E_c}{a} \sum_{k=1}^{N_c} \sin^2 \lambda x_k$$

$$L_{24} = \left(\frac{B_{66}}{a} + \frac{B_{12}}{a}\right) \frac{n}{\alpha}$$

$$\begin{aligned}
 L_{25} &= B_{66} - \left( \frac{B_{22} n^2}{a^2} + \frac{H_{44} 1}{a^2 \alpha^2} \right) \frac{T_4}{T_3} \\
 L_{31} &= -\frac{A_{12}}{a} \\
 L_{32} &= -\left( \frac{A_{22}}{a^2} + \frac{H_{44}}{a^2} \right) \frac{n T_4}{\alpha^2 T_3} \\
 L_{33} &= H_{66} - \left( \frac{H_{44} n^2}{a^2 \alpha^2} + \frac{A_{22} 1}{a^2 \alpha^2} \right) \frac{T_4}{T_3} + \left( \frac{2n^4 \pi^2 I_{oc} E_c}{a} + \frac{2\pi^2 A_c E_c}{a} \right) \sum_{k=1}^{N_c} \sin^2 \lambda x_k \\
 &\quad + \frac{2n^2 \pi^2 \lambda^2 G_c J_c}{a} \sum_{k=1}^{N_c} \cos^2 \lambda x_k + \frac{1}{2} L N_a \pi \lambda^4 I_{oa} (E_s) \\
 &\quad + \frac{4n^2 \pi^2 A_c E_c z_c}{a^2} \sum_{k=1}^{N_c} \sin^2 \lambda x_k + \frac{PL\pi (n^2 - 1)}{4} \\
 L_{34} &= \left( H_{55} - \frac{B_{12}}{a} \right) \frac{1}{\alpha} \\
 L_{35} &= \left( \frac{H_{44}}{a} + \frac{B_{22}}{a^2} \right) \frac{n T_4}{\alpha^2 T_3} \\
 L_{41} &= B_{11} a \alpha^2 T_1 - \frac{B_{66}}{a} n^2 T_2 \\
 L_{42} &= (B_{12} + B_{66}) n T_2 \\
 L_{43} &= (B_{12} - H_{55} a) T_2 \\
 L_{44} &= D_{11} a \alpha T_1 - \left( \frac{D_{66} n^2}{a} \frac{1}{\alpha} - H_{55} a \frac{1}{\alpha} \right) T_2 \\
 L_{45} &= (D_{12} + D_{66}) n T_2 \\
 L_{51} &= -(B_{12} + B_{66}) \alpha n T_3 \\
 L_{52} &= B_{66} a \alpha T_3 - \left( \frac{B_{22} n^2}{a} \frac{1}{\alpha} - H_{44} \frac{1}{\alpha} \right) T_4 \\
 L_{53} &= \left( -\frac{B_{22}}{a} + H_{44} \right) \frac{n T_4}{\alpha} \\
 L_{54} &= -(D_{12} + D_{66}) n T_3 \\
 L_{55} &= D_{66} a \alpha T_3 - \left( \frac{D_{22} n^2}{a} \frac{1}{\alpha} + H_{44} a \frac{1}{\alpha} \right) T_4 \\
 \alpha &= \frac{\lambda}{L} \\
 \lambda &= m\pi \\
 T_1 &= \alpha_1 (\cosh \lambda - 1) - \alpha_2 (\cos \lambda - 1) - \sigma (\alpha_3 \sinh \lambda + \alpha_4 \sin \lambda) \\
 T_2 &= \alpha_1 (\cosh \lambda - 1) - \alpha_2 (\cos \lambda - 1) - \sigma (\alpha_3 \sinh \lambda - \alpha_4 \sin \lambda) \\
 T_3 &= \alpha_1 \sinh \lambda - \alpha_2 \sin \lambda - \sigma (\alpha_3 (\cosh \lambda - 1) - \alpha_4 (\cos \lambda - 1)) \\
 T_4 &= \alpha_1 \sinh \lambda + \alpha_2 \sin \lambda - \sigma (\alpha_3 (\cosh \lambda - 1) + \alpha_4 (\cos \lambda - 1))
 \end{aligned}$$

where:

$$\begin{aligned}
 I_{os} &= I_a + z_a^2 A_a, & I_{or} &= I_c + z_c^2 A_c \\
 J_c &= \frac{1}{3} b_c h_c^3, & J_a &= \frac{1}{3} b_a h_a^3
 \end{aligned}$$

## References

- [1] H.S. Shen, T.Y. Chen, Buckling and postbuckling behavior of cylindrical shells under combined external pressure and axial compression, *Thin-Walled Struct.* 12 (1991) 321–334.
- [2] P.M. Naghdi, A survey of recent progress in the theory of elastic shells, *Appl. Mech. Rev.* 9 (1956) 365–368.
- [3] C.W. Bert, Dynamics of composite and sandwich panels – parts I and II, *Shock Vib. Dig.* 8 (1976) 37–48.
- [4] E. Reissner, Stress-strain relations in the theory of thin elastic shells, *J. Math. Phys.* 31 (1952) 109–119.
- [5] J.A. Zukas, J.R. Vinson, Laminated transversely isotropic cylindrical shells, *J. Appl. Mech.* 38 (1971) 400–407.
- [6] S.B. Dong, K.S. Pister, R.L. Taylor, On the theory of laminated anisotropic shells and plates, *J. Aerosp. Sci.* 29 (1962) 969–975.
- [7] S.B. Dong, On a laminated orthotropic shell theory including transverse shear deformation, *J. Appl. Mech.* 39 (1972) 1091–1096.
- [8] J.N. Reddy, C.F. Liu, A higher-order shear deformation theory of laminated elastic shells, *Int. J. Eng. Sci.* 23 (1985) 319–330.
- [9] J.N. Reddy, Bending of laminated anisotropic shells by a shear deformable finite element, *Fibre Sci. Technol.* 17 (1982) 9–24.
- [10] H.S. Shen, T.Y. Chen, Buckling and post-buckling behavior of cylindrical shells under combined external pressure and axial compression, *Thin-Walled Struct.* 12 (1991) 321–334.
- [11] M. Barush, J. Singer, Effect of eccentricity of stiffeners on the general instability of stiffened cylindrical shells under hydrostatic pressure, *J. Mech. Eng. Sci.* 5 (1963) 23–27.
- [12] H.S. Shen, P. Zhou, T.Y. Chen, Post-buckling analysis of stiffened cylindrical shells under combined external pressure and axial compression, *Thin-Walled Struct.* 15 (1993) 43–63.
- [13] S. Sridharan, M. Zeggane, Stiffened plates and cylindrical shells under interactive buckling, *Finite Elem. Anal. Des.* 38 (2001) 155–178.
- [14] Ji Zhen-yi, Yeh Kei-yuan, General solution for nonlinear buckling of nonhomogeneous axial symmetric ring- and stringer-stiffened cylindrical shells, *Comput. Struct.* 34 (4) (1990) 585–591.
- [15] M. Sadeghifar, M. Bagheri, A.A. Jafari, Buckling analysis of stringer-stiffened laminated cylindrical shells with nonuniform eccentricity, *Arch. Appl. Mech.* 81 (2011) 875–886.
- [16] J.N. Reddy, *Mechanics of Laminated Composite Plates and Shells, Theory Anal.*, CRC Press LLC, Boca Raton, FL, USA, 2004.
- [17] D.O. Brush, B.O. Almroth, *Buckling of Bars, Plates and Shells*, McGraw-Hill, New York, 1975.